JOURNAL OF COMPUTATIONAL PHYSICS 100, 17–24 (1992)

An Algorithm for Calculating Intramolecular Angle-Dependent Forces on Vector Computers

J. H. DUNN,* S. G. LAMBRAKOS,† P. G. MOORE,† AND M. NAGUMO‡

*Code 5842, †Code 6320, and ‡Code 6190, Naval Research Laboratory, Washington, D.C. 20375-5000

Received March 23, 1990; revised January 14, 1991

We describe an approach based on projection methods for the calculation of angle-bending and torsional forces in molecular dynamics simulations. These forces are important in molecular dynamics simulations of systems containing polyatomic molecules. A significant speedup can be achieved using projection methods, because they require fewer high-cost operations than traditional cross-product methods. Initial tests on a Cray X-MP show factors of 7 and 2.5 increase in speed for the calculation of angle-bending and torsional forces, respectively, relative to a comparable cross-product formulation. Our analysis of projection methods for calculating intramolecular angle-dependent forces provides a framework for the development of efficient programming structures.

I. INTRODUCTION

In molecular dynamics simulations of systems consisting of polyatomic molecules, e.g., polymers or lipids, modelling the energy transfer between intermolecular and intramolecular degrees-of-freedom is necessary if accurate molecular parameters, e.g., order parameters and self-diffusion rates, are to be extracted [1]. In the classical representation [2], intramolecular degrees-of-freedom are decomposed into four general types of interactions for which both ab initio quantum mechanical and experimental, e.g., spectroscopic, data can be obtained. These interactions are: bond-stretching, bond-angle-bending, torsion, and out-of-plane wag. We do not treat out-of-plane wag in this analysis, since we concern ourselves only with linearly linked molecules. Further, out-of-plane wag may be handled in a manner similar to torsion.

While the calculation of bond-stretching is easily vectorized, there are inherent limitations on the vectorization of angle-bending and torsional force evaluations. These are due to the many-body nature of the forces, as well as to the multiple-linkage between particles. Given these inherent limitations, the task, then, is to seek optimal partitioning of the problem for efficient vector computation.

In addition to the problem of multiple-linkage, the computational cost of evaluating angle-dependent forces is relatively high, since these forces are non-central and, therefore, require addition operations to evaluate their direction cosines. Typical procedures for calculating angle-dependent forces involve cross-products. Cross-product procedures can be vectorized by using *gather–scatter* operations, which address the linkage problem by using linked-lists; however, projection methods are more efficient. Projection methods require fewer high-cost operations, e.g., square roots and divisions, and incorporate efficient programming structures for vector computation. Initial tests show factors of 7 and 2.5 increase in speed for the calculation of angle-bending and torsional forces, respectively, relative to a comparable cross-product formulation on a Cray X-MP.

We describe in this paper a method for calculating angle-dependent forces in molecular dynamics simulations that represents an efficient partitioning of the problem for vector computation. The paper is organized as follows. In Section II, we present the formulation of the problem. In Section III, we describe our algorithm for numerically evaluating the forces. Section IV presents timings and the results of comparisons of our method to traditional methods.

II. FORMULATION

A. *Background*

In the theory of molecular vibrations [2], internal degrees of freedom of a linearly linked molecule, e.g., decane, ($C_{10}H_{22}$), are generally decomposed into three independent modes: bond-stretching, bond-angle-bending, and torsion. These are 2-, 3- and 4-body interactions, respectively. Vibrational and angle-bending modes are harmonic in nature and have characteristic frequencies which are high relative to those of torsional and intermolecular modes. They are usually represented by a potential function of the form

$$V(q) = \tfrac{1}{2}\kappa q^2, \tag{1}$$

0021-9991/92 $5.00

where κ is a stiffness parameter and q is a generalized coordinate with its origin at the equilibrium point. In contrast, torsion is a relatively low-frequency mode and can be represented by a function of the form

$$V(\phi) = \sum_{i=0}^{n} \alpha_i \cos^i(\phi), \tag{2}$$

where the coefficients, α_i, are determined empirically and ϕ is the dihedral angle (see Fig. 2) specified in a coordinate system internal to the 4-body system. Note that Eq. (2) is the power series rather than the Fourier series definition.

There has been considerable interest in the decoupling of internal and rotational modes in the study of molecular vibrations [2–4]. Rotational modes are those which involve the rotation of the entire molecule about a principal axis of inertia. This interest is due to the computational difficulty associated with calculating molecular motions, i.e., solving the wave equation, when the terms which depend on rotation cannot be separated from those which depend on internal degrees-of-freedom. Therefore, some effort has been spent in defining an internal coordinate system in which they are approximately decoupled. We require that our simulation conserve total energy, as opposed to readjusting the kinetic energy by rescaling the center-of-mass velocities. Since the integration of differential equations depending on higher frequency modes generally requires a smaller timestep, we require that the internal modes be decoupled from the rotational modes, i.e., that the equations of motion of the center-of-mass not be stiff. This allows us to use a larger timestep for intermolecular modes. We will, therefore, define an internal coordinate system where rotation and vibration are approximately decoupled, and show that, in the case of a simulation where only torsional degrees-of-freedom are taken into account, they are completely decoupled.

Let $\mathbf{r}_\alpha$ be the position of the αth particle in the internal coordinate system and m_α be its mass. Further, let this coordinate system be fixed at the center-of-mass of the n-body system, i.e., satisfy the condition

$$\sum_{\alpha=1}^{n} m_\alpha \mathbf{r}_\alpha = \mathbf{0}. \tag{3}$$

Let the equilibrium positions of the vibrational modes in this system be denoted by $\mathbf{d}_\alpha$ and correspond to the positions where all internal contributions to the potential energy are zero.

There are two conditions, then, that must be satisfied in order to decouple the rotational and intramolecular modes. First, the internal coordinates must be chosen such that the angular momentum of the equilibrium configuration is zero [4],

$$\sum_{\alpha=1}^{n} m_\alpha \mathbf{d}_\alpha \times \mathbf{v}_\alpha = \mathbf{0}, \tag{4}$$

where $\mathbf{v}_\alpha$ is the velocity in the internal coordinate system. Second, all intramolecular frequencies must be of the same order of magnitude. Further, they must be large enough such that first-order kinetic energy terms in angular momentum are of the same order of magnitude or less than second-order terms [3] in the Hamiltonian. This is equivalent to the condition that vibrational amplitudes be small enough that the inertial tensor is, essentially, a constant of the motion [3]. That is, each particle of the n-body system must remain close to $\mathbf{d}_\alpha$. The form of the kinetic energy is, ignoring center-of-mass momentum [2],

$$2T = \omega \cdot \sum_{\alpha=1}^{n} (m_\alpha \mathbf{v}_\alpha \times \mathbf{r}_\alpha) + \sum_{\alpha=1}^{n} (\omega \times \mathbf{r}_\alpha)^2 + \sum_{\alpha=1}^{n} m_\alpha v_\alpha^2, \tag{5}$$

where ω is the rotational velocity of the n-body system. The first- and second-order terms are the first and second terms in Eq. (5), respectively.

The condition, Eq. (4), is satisfied by using the center-of-momentum system for the internal coordinate system. This choice acts as an implicit holonomic constraint on the rotation and translation of the center-of-mass. We ensure that the second condition is satisfied by constraining the interparticle distances and bond-angles instead of using a stiff harmonic potential to model bond-stretching and angle-bending. We use for this the MSHAKE [5, 6] constraint algorithm. Given Eq. (4), the first-order term in Eq. (5) reduces to $\omega \cdot \sum_{\alpha=1}^{n} (m_\alpha \mathbf{v}_\alpha \times \mathbf{q}_\alpha)$, where $\mathbf{q} = \mathbf{r} - \mathbf{d}$. Since we consider only the torsional degree-of-freedom, $\mathbf{v}_\alpha = \dot{\mathbf{q}}_\alpha$ so that $\mathbf{v}_\alpha \times \mathbf{r}_\alpha = 0$ for all α. This means that both linear and angular momenta are constants of the motion, i.e., zero in the internal coordinate system of each molecule. In a simulation with complete detail, the bond-angle-bending potential would be modelled by a stiff harmonic potential. Since we assume infinitesimal displacements, the internal degrees-of-freedom are nearly orthogonal. Therefore, the first-order term in angular momentum involves only cross-terms between vibrational velocities and displacements, which will be small. Next, we define the angle-bending and torsional forces.

B. *Angle-Bending Force Definition*

Angle-bending is equivalent [2] to the set of (infinitesimal) displacements $\mathbf{s}_{t1}$, $\mathbf{s}_{t2}$, and $\mathbf{s}_{t3}$ shown in

Fig. 1. We will refer to particles 1 and 2 as the end-particles, and to particle 3 as the pivot-particle. The magnitudes s_{t1} and s_{t2} are inversely proportional to the lengths of the corresponding bonds,

$$s_{t1} = r_{31}^{-1} \quad \text{and} \quad s_{t2} = r_{32}^{-1}. \tag{6}$$

Further, displacements must satisfy the relation

$$\mathbf{s}_{t3} = -\mathbf{s}_{t1} - \mathbf{s}_{t2}. \tag{7}$$

The **s** vectors are [3]

$$\mathbf{s}_{t1} = \frac{1}{r_{31}} \mathbf{e}_{31} \times \frac{(\mathbf{e}_{31} \times \mathbf{e}_{32})}{\sin\theta}, \tag{8}$$

$$\mathbf{s}_{t2} = \frac{1}{r_{32}} \mathbf{e}_{32} \times \frac{(\mathbf{e}_{32} \times \mathbf{e}_{31})}{\sin\theta}, \tag{9}$$

$$\mathbf{s}_{t3} = \frac{(r_{31} - r_{32}\cos\theta)\,\mathbf{e}_{31} + (r_{32} - r_{31}\cos\theta)\,\mathbf{e}_{32}}{r_{31} r_{32} \sin\theta}, \tag{10}$$

where $\mathbf{e}_{ab}$ is the unit vector pointing from atom a to atom b, and θ is the angle between two unit vectors (see Fig. 1a).

The forces that produce angle-bending act along the **s** vectors and are proportional to their length. The constants of proportionality are given by $F(\theta) = -(dV(\theta)/d\theta)$, where $V(\theta)$ is the angle-bending potential, Eq. (1). The magnitudes of the forces applied to the end-particles, $\mathbf{f}_1$ and $\mathbf{f}_2$, respectively, are derived from Eq. (5):

$$f_1 = \frac{F(\theta)}{r_{31}} \quad \text{and} \quad f_2 = \frac{F(\theta)}{r_{32}}. \tag{11}$$

We may reformulate the problem by noting that the **s** vectors lie in the plane of the particles and are orthogonal to the corresponding bonds. Therefore the problem reduces projecting the line of centers between particles 1 and 2, $\mathbf{r}_{21}$, into the spaces orthogonal to the bonds. We define a force, $\mathbf{f}'$, in the direction of $\mathbf{r}_{21}$ such that the magnitude of its components normal to $\mathbf{r}_{31}$ and $\mathbf{r}_{32}$ are precisely those of the angle-bending force (see Fig. 1b). The force is

$$\mathbf{f}' = -\left(\frac{dV(\theta)}{d\theta}\right) \frac{1}{\sin\theta} \frac{\mathbf{r}_{21}}{r_{31} r_{32}}. \tag{12}$$

We then define a projection operator [7]

$$P(\mathbf{v}) = I - \frac{\mathbf{v}\mathbf{v}^{\mathrm{T}}}{\|\mathbf{v}\|^2}. \tag{13}$$

The forces on particles 1, 2, and 3 are

$$\mathbf{f}_1 = P(\mathbf{r}_{31})\,\mathbf{f}', \tag{14a}$$

$$\mathbf{f}_2 = -P(\mathbf{r}_{32})\,\mathbf{f}', \tag{14b}$$

and

$$\mathbf{f}_3 = -\mathbf{f}_1 - \mathbf{f}_2. \tag{14c}$$

It is easy to verify that the expressions given in Eqs. (14) are equivalent to the corresponding expressions derived from Eqs. (8)–(10).

C. *Torsional Force Definition*

The potential energy of a molecule having linearly linked sequences of four or more particles has contributions from a term that is a function of the torsion angle, ϕ (see Fig. 3) between the planes defined by atoms (1, 2, 3) and (2, 3, 4) of the sequence, where

$$\cos\phi = \frac{(\mathbf{e}_{12} \times \mathbf{e}_{23}) \cdot (\mathbf{e}_{23} \times \mathbf{e}_{34})}{\sin\theta_2 \sin\theta_3}. \tag{15}$$

The displacement vectors that define torsion are [2] (see Fig. 2)

$$\mathbf{s}_{t1} = -\frac{\mathbf{e}_{12} \times \mathbf{e}_{23}}{r_{12} \sin^2\theta_2}, \tag{16}$$

$$\mathbf{s}_{t2} = \frac{r_{23} - r_{12}\cos\theta_2}{r_{23} r_{12} \sin\theta_2} \frac{\mathbf{e}_{12} \times \mathbf{e}_{23}}{\sin\theta_2} + \frac{\cos\theta_3}{r_{23}\sin\theta_3} \frac{\mathbf{e}_{43} \times \mathbf{e}_{32}}{\sin\theta_3}, \tag{17}$$

$$\mathbf{s}_{t3} = [(14)(23)]\,\mathbf{s}_{t2}, \tag{18}$$

$$\mathbf{s}_{t4} = [(14)(23)]\,\mathbf{s}_{t1}. \tag{19}$$

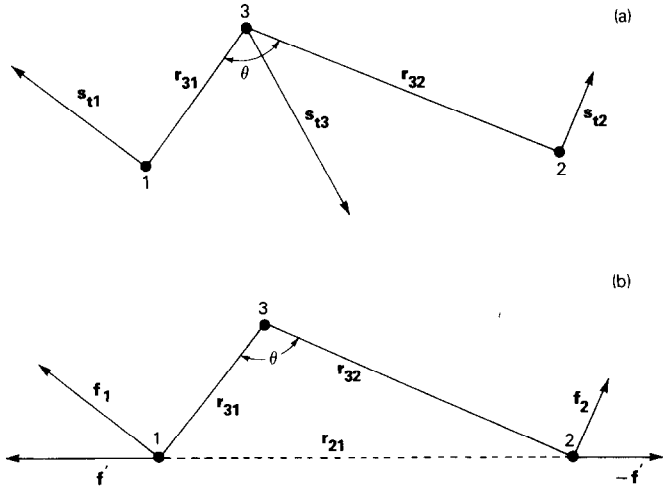

FIG. 1. (a) Angle-bending displacements; (b) projection-based angle-bending algorithm vectors.

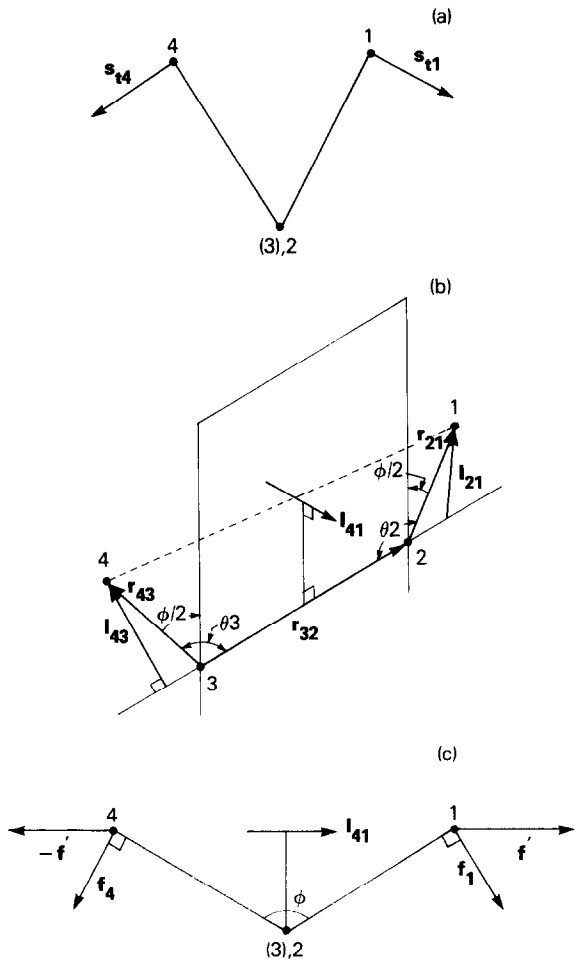

FIG. 2. (a) Torsion displacements; (b) l vectors normal to the pivot-bond; (c) torsional forces on the end-particles.

The expressions in square brackets indicate the permutation of indices; e.g., (23) means that every instance of 2 should be replaced by 3 and vice versa. The $\mathbf{s}$ vectors must satisfy the condition

$$\mathbf{s}_{t1}+\mathbf{s}_{t2}+\mathbf{s}_{t3}+\mathbf{s}_{t4}=\mathbf{0}. \tag{20}$$

The magnitude of the torsional force on particle i is given by

$$F(\phi)_i=\left(\frac{-dV(\phi)}{d\phi}\right)s_i. \tag{21}$$

We reformulate this problem by noting that the torsional forces on the end-particles are orthogonal to the bonds between the pivot-particles and the end-particles, i.e., $\mathbf{f}_1 \perp \mathbf{r}_{21}$ and $\mathbf{f}_4 \perp \mathbf{r}_{43}$. They must also be normal to the pivot-vector, i.e., $\{\mathbf{f}_1, \mathbf{f}_1\} \perp \mathbf{r}_{32}$. As in the previous section, we define a force $\mathbf{f}'$ that is directed along the projection of the line of centers between the end-particles normal to the pivot-vector (Fig. 2c),

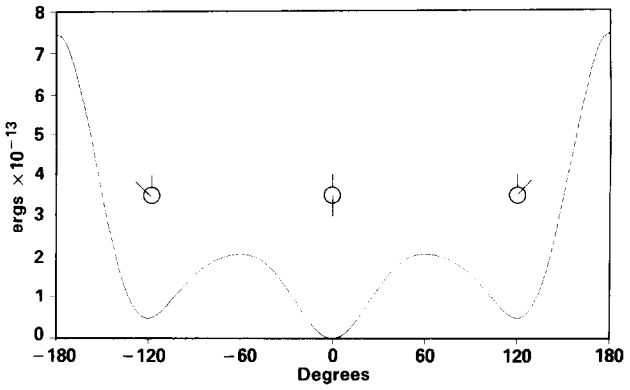

FIG. 3. The torsional potential energy. Insets show the *trans* conformation at 0° and the *gauche*$^+$ and *gauche*$^-$ conformations at $\pm 120°$, respectively.

$$\mathbf{f}'=-\frac{dV(\phi)}{d\phi}\frac{1}{\sin\phi}\frac{l_{41}}{l_{21}l_{43}}, \tag{22}$$

where l_{ab} are defined as the components of $\mathbf{r}_{ab}$ normal to the pivot vector:

$$l_{21}=P(\mathbf{r}_{32})\,\mathbf{r}_{21}, \tag{23a}$$

$$l_{43}=P(\mathbf{r}_{32})\,\mathbf{r}_{43}, \tag{23b}$$

and

$$l_{41}=P(\mathbf{r}_{32})\,\mathbf{r}_{41}. \tag{23c}$$

The torsional forces on particles 1 and 4 are

$$\mathbf{f}_1=P(l_{21})\,\mathbf{f}' \tag{24a}$$

and

$$\mathbf{f}_4=P(l_{43})\,\mathbf{f}'. \tag{24b}$$

The compensatory forces on particles 2 and 3 are given by Eqs. (16) and (17), which yield, after simplifying $\cos(\theta_i)$ terms,

$$\mathbf{f}_2=\mathbf{f}_1-\left(\frac{\mathbf{r}_{32}\cdot\mathbf{r}_{21}}{\|\mathbf{r}_{32}\|^2}\right)\mathbf{f}_1+\left(\frac{\mathbf{r}_{32}\cdot\mathbf{r}_{43}}{\|\mathbf{r}_{32}\|^2}\right)\mathbf{f}_4, \tag{25a}$$

$$\mathbf{f}_3=\mathbf{f}_4-\left(\frac{\mathbf{r}_{32}\cdot\mathbf{r}_{43}}{\|\mathbf{r}_{32}\|^2}\right)\mathbf{f}_4+\left(\frac{\mathbf{r}_{32}\cdot\mathbf{r}_{21}}{\|\mathbf{r}_{32}\|^2}\right)\mathbf{f}_1. \tag{25b}$$

The vectors $\mathbf{f}_2$ and $\mathbf{f}_3$ are parallel to the plane normal to $\mathbf{r}_{32}$, but their directions are not easily displayed.

These force definitions are easily generalized to the case of

more than one end-particle, e.g., F_3C-BF_2. In the general case, particle 1 may be replaced by n particles of one type, denoted $\mathbf{r}_{21}^i$, and particle 4 by m particles of another, denoted $\mathbf{r}_{43}^i$. In this case, the torsional forces are [8]:

$$\mathbf{f}_1 = \frac{1}{n} P(\boldsymbol{l}_{21})\,\mathbf{f}' \tag{26a}$$

and

$$\mathbf{f}_4 = \frac{1}{m} P(\boldsymbol{l}_{43})\,\mathbf{f}'. \tag{26b}$$

The forces on particles 2 and 3 are then linear combinations of the contributions from all the end-members:

$$\mathbf{f}_2 = -\frac{1}{n}\sum_{i=1}^{n}\left[\mathbf{f}_1^i - \left(\frac{\mathbf{r}_{32}\cdot\mathbf{r}_{21}^i}{\|\mathbf{r}_{32}\|^2}\right)\mathbf{f}_1^i\right] + \frac{1}{m}\sum_{j=1}^{m}\left(\frac{\mathbf{r}_{32}\cdot\mathbf{r}_{43}^j}{\|\mathbf{r}_{32}\|^2}\right)\mathbf{f}_4^j, \tag{27a}$$

$$\mathbf{f}_3 = -\frac{1}{m}\sum_{i=1}^{m}\left[\mathbf{f}_4^i - \left(\frac{\mathbf{r}_{32}\cdot\mathbf{r}_{43}^i}{\|\mathbf{r}_{32}\|^2}\right)\mathbf{f}_4^i\right] + \frac{1}{n}\sum_{j=1}^{n}\left(\frac{\mathbf{r}_{32}\cdot\mathbf{r}_{21}^j}{\|\mathbf{r}_{32}\|^2}\right)\mathbf{f}_1^j. \tag{27b}$$

D. *Mechanical Equivalence of the Methods*

In this section, we state formally the mechanical equivalence of the projection methods to the cross-product method and present a rigorous proof of this equivalence. Specifically, the forces calculated by the projection method are the same as those calculated by the cross-product method, i.e.,

$$\mathbf{f}_1^p = \mathbf{f}_1^{cp},\quad \mathbf{f}_2^p = \mathbf{f}_2^{cp},\quad \mathbf{f}_3^p = \mathbf{f}_3^{cp},\quad \mathbf{f}_4^p = \mathbf{f}_4^{cp}, \tag{28}$$

where the superscripts cp and p designate cross-product and projection, respectively, and the subscripts designate the particle on which the forces act.

First, we note that $\mathbf{f}_1^p = \mathbf{f}_1^{cp}$ if and only if $\mathbf{f}_1^p/\|\mathbf{f}_1^p\| = \mathbf{f}_1^{cp}/\|\mathbf{f}_1^{cp}\|$ and $\|\mathbf{f}_1^p\| = \|\mathbf{f}_1^{cp}\|$. Further, we note that $\mathbf{f}_1^p/\|\mathbf{f}_1^p\| = \mathbf{f}_1^{cp}/\|\mathbf{f}_1^{cp}\|$ if and only if $\mathbf{f}_1'/\|\mathbf{f}_1^p\|$ is parallel to $\mathbf{f}_1^{cp}/\|\mathbf{f}_1^{cp}\|$, and $(\mathbf{f}_1^p/\|\mathbf{f}_1^p\|)\cdot(\mathbf{f}_1^{cp}/\|\mathbf{f}_1^{cp}\|) > 0$. Thus the equality $\mathbf{f}_1^p = \mathbf{f}_1^{cp}$ is verified if we show the validity of the conditions: (a) $\mathbf{f}_1^p/\|\mathbf{f}_1^p\|$ is parallel to $\mathbf{f}_1^{cp}/\|\mathbf{f}_1^{cp}\|$; (b) $(\mathbf{f}_1^p/\|\mathbf{f}_1^p\|)\cdot(\mathbf{f}_1^{cp}/\|\mathbf{f}_1^{cp}\|) > 0$; and (c) $\|\mathbf{f}_1^p\| = \|\mathbf{f}_1^{cp}\|$.

Condition (a) follows, since

$$\frac{\mathbf{f}_1^{cp}}{\|\mathbf{f}_1^{cp}\|} = -\frac{\mathbf{e}_{12}\times\mathbf{e}_{23}}{\sin\theta_2}, \tag{29}$$

which is orthogonal to both $\mathbf{e}_{12}$ and $\mathbf{e}_{23}$. Since the vector $\mathbf{e}_{12}$ is not parallel to $\mathbf{e}_{23}$, the vectors $\mathbf{e}_{12}$ and $\mathbf{e}_{23}$ define a plane P such that $\mathbf{f}_1^{cp}/\|\mathbf{f}_1^{cp}\|$ is orthogonal to P. Thus it follows that if $\mathbf{f}_1^p/\|\mathbf{f}_1^p\|$ is orthogonal to P, then $\mathbf{f}_1^p/\|\mathbf{f}_1^p\|$ is parallel to $\mathbf{f}_1^{cp}/\|\mathbf{f}_1^{cp}\|$. From Eq. (24a),

$$\mathbf{f}_1^p = \mathbf{f}_1' - \boldsymbol{l}_{21}\frac{\boldsymbol{l}_{21}^{\mathrm{T}}\mathbf{f}_1'}{\|\boldsymbol{l}_{21}\|^2}, \tag{30}$$

and from Eq. (23a), $\boldsymbol{l}_{21} = \mathbf{r}_{21} - \mathbf{r}_{32}(\mathbf{r}_{32}^{\mathrm{T}}\mathbf{r}_{21}/\|\mathbf{r}_{32}\|^2)$ and is orthogonal to $\mathbf{e}_{23}$. Further, $\mathbf{f}_1'$ is parallel to $\boldsymbol{l}_{41}$, and $\boldsymbol{l}_{41} = \mathbf{r}_{41} - \mathbf{r}_{32}(\mathbf{r}_{32}^{\mathrm{T}}\mathbf{r}_{41}/\|\mathbf{r}_{32}\|^2)$ and is orthogonal to $\mathbf{e}_{23}$. Thus, $\mathbf{f}_1^p$ is orthogonal to $\mathbf{e}_{23}$, since it is a linear combination of two vectors orthogonal to $\mathbf{e}_{23}$. Finally, since $\boldsymbol{l}_{21}$ is parallel to $\mathbf{e}_{12}$ and (by Eq. (30)) $\mathbf{f}_1^p$ is orthogonal to $\boldsymbol{l}_{21}$, $\mathbf{f}_1^p$ is orthogonal to $\mathbf{e}_{12}$. Therefore, $\mathbf{f}_1^p$ is orthogonal to P and $\mathbf{f}_1^p/\|\mathbf{f}_1^p\|$ is parallel to $\mathbf{f}_1^{cp}/\|\mathbf{f}_1^{cp}\|$.

Next, condition (b) follows, since

$$\frac{\mathbf{f}_1^{cp}}{\|\mathbf{f}_1^{cp}\|}\cdot\frac{\mathbf{f}_1^p}{\|\mathbf{f}_1^p\|} = -F(\phi)^2\frac{\mathbf{e}_{12}\times\mathbf{e}_{23}}{\sin\theta_2}\frac{\zeta}{\sin\phi}\cdot\left[\mathbf{r}_{41} - \mathbf{r}_{32}\frac{\mathbf{r}_{32}^{\mathrm{T}}\mathbf{r}_{41}}{\|\mathbf{r}_{32}\|^2} - \frac{\mathbf{r}_{21}\mathbf{r}_{32}^{\mathrm{T}}}{\|\mathbf{r}_{21}\|^2}\right], \tag{31}$$

where $\zeta = [\|\boldsymbol{l}_{34}\|\,\|\boldsymbol{l}_{21}\|]^{-1}$. Further, since $F(\phi)^2\zeta \geqslant 0$ and the forces are trivially equal if they are all zero, we ignore these terms and obtain

$$-\frac{\mathbf{e}_{12}\times\mathbf{e}_{23}}{\sin\theta_2\sin\phi}\cdot[\mathbf{r}_{41} - \lambda_1\mathbf{r}_{32} - \lambda_2\mathbf{r}_{21}]. \tag{32}$$

But $(\mathbf{e}_{12}\times\mathbf{e}_{23})\cdot\mathbf{r}_{32} = 0$ and $(\mathbf{e}_{12}\times\mathbf{e}_{23})\cdot\mathbf{r}_{21} = 0$, so the expression simplifies to

$$-\frac{\mathbf{e}_{12}\times\mathbf{e}_{23}}{\sin\theta_2}\cdot\frac{\mathbf{r}_{41}}{\sin\phi} = \frac{\|\mathbf{r}_{41}\|\sin\alpha}{\sin\phi}, \tag{33}$$

where α is the angle between $\mathbf{f}_1'$ and $\boldsymbol{l}_{21}$ (see Fig. 2c). Finally, noting that $(\|\mathbf{r}_{41}\|\sin\alpha)/\sin\phi = (\|\mathbf{r}_{41}\|\,\|\boldsymbol{l}_{34}\|)/\|\boldsymbol{l}_{41}\| > 0$, it follows that $(\mathbf{f}_1^p/\|\mathbf{f}_1^p\|)\cdot(\mathbf{f}_1^{cp}/\|\mathbf{f}_1^{cp}\|) > 0$.

Finally, condition(c) is verified as follows: We have

$$\|\mathbf{f}_1^{cp}\| = \frac{|F(\phi)|}{\|\mathbf{r}_{12}\|\sin\theta_2}, \tag{34}$$

$$\|\mathbf{f}_1^p\| = \|\mathbf{f}_1'\|\sin\alpha, \tag{35}$$

and (by the law of sines) $\sin\alpha = (\|\boldsymbol{l}_{34}\|\sin\phi)/\|\boldsymbol{l}_{41}\|$. Further, substituting

$$\|\mathbf{f}_1'\| = \frac{1}{\sin\phi}\frac{\|\boldsymbol{l}_{41}\|}{\|\boldsymbol{l}_{21}\|\,\|\boldsymbol{l}_{34}\|}F(\phi)| \tag{36}$$

and the above expression for $\sin\alpha$ into Eq. (35) yields

$\|\mathbf{f}_1^p\| = |F(\phi)|/\|\boldsymbol{l}_{21}\|$. Finally, since $\|\boldsymbol{l}_{21}\| = \|\mathbf{r}_{21}\| \sin\theta_2$, it follows that $\|\mathbf{f}_1^p\| = |F(\phi)|/(\|\mathbf{r}_{21}\| \sin\theta_2)$ and $\mathbf{f}_1^p = \mathbf{f}_1^{cp}$. The equality $\mathbf{f}_4^{cp} = \mathbf{f}_4^p$ is verified by replacing particles 1 and 2 with particles 3 and 4, respectively, and θ_2 with θ_3 in the above development.

The equality $\mathbf{f}_2^p = \mathbf{f}_2^{cp}$ is verified as follows: We note that $\mathbf{f}_2^p = \lambda_1^p \mathbf{f}_1^p + \lambda_2^p \mathbf{f}_4^p$ and $\mathbf{f}_2^{cp} = \lambda_1^{cp} \mathbf{f}_1^{cp} + \lambda_2^{cp} \mathbf{f}_4^{cp}$ and are equal if and only if $\mathbf{f}_1^p = \mathbf{f}_1^{cp}$, $\mathbf{f}_4^p = \mathbf{f}_4^{cp}$, $\lambda_1^p = \lambda_1^{cp}$, and $\lambda_2^p = \lambda_2^{cp}$. Since the equalities $\mathbf{f}_1^p = \mathbf{f}_1^{cp}$ and $\mathbf{f}_4^p = \mathbf{f}_4^{cp}$ have been verified, it is sufficient to show that $\lambda_1^p = \lambda_1^{cp}$ and $\lambda_2^p = \lambda_2^{cp}$. It follows from Eq. (17) that $\lambda_1^{cp} = -(1 - (\|\mathbf{r}_{21}\|/\|\mathbf{r}_{32}\|) \cos\theta_2)$. Now, since

$$-\cos\theta_2 = \left\| \mathbf{r}_{32} \frac{\mathbf{r}_{32}^{\mathrm{T}} \mathbf{r}_{21}}{\|\mathbf{r}_{32}\|^2} \right\| (\|\mathbf{r}_{21}\|)^{-1}, \tag{37}$$

$-(\|\mathbf{r}_{21}\|/\|\mathbf{r}_{32}\|) \cos\theta_2 = (\mathbf{r}_{32}^{\mathrm{T}} \mathbf{r}_{21})/\|\mathbf{r}_{32}\|^2$. Finally, it follows from Eq. (25a) that $\lambda_1^p = -(1 + (\mathbf{r}_{32}^{\mathrm{T}} \mathbf{r}_{21})/\|\mathbf{r}_{32}\|^2)$ and $\lambda_1^p = \lambda_1^{cp}$. Similarly, since $\lambda_2^{cp} = -(\|\mathbf{r}_{34}\|/\|\mathbf{r}_{32}\|) \cos\theta_3$ and

$$-\cos\theta_3 = \left\| \mathbf{r}_{32} \frac{\mathbf{r}_{32}^{\mathrm{T}} \mathbf{r}_{34}}{\|\mathbf{r}_{32}\|^2} \right\| (\|\mathbf{r}_{34}\|)^{-1}, \tag{38}$$

it follows that $-(\|\mathbf{r}_{34}\|/\|\mathbf{r}_{32}\|) \cos\theta_3 = (\mathbf{r}_{32}^{\mathrm{T}} \mathbf{r}_{34})/\|\mathbf{r}_{32}\|^2$. Finally, since $\lambda_2^p = (\mathbf{r}_{32}^{\mathrm{T}} \mathbf{r}_{34})/\|\mathbf{r}_{32}\|^2$, it follows that $\lambda_2^p = \lambda_2^{cp}$ and $\mathbf{f}_2^p = \mathbf{f}_2^{cp}$. The equality $\mathbf{f}_3^p = \mathbf{f}_3^{cp}$ is verified by noting that the terms in $\cos\theta_2$ and $\cos\theta_3$ in Eq. (18) are the same as those in Eq. (17).

III. ALGORITHMIC IMPLEMENTATION

A. *Bond-Angle-Bending*

The bond-angle-bending algorithm consists of three phases. In the first, the system coordinates and masses of the particles are GATHERed and the center-of-momentum coordinates are computed (see Fig. 4). Next, the direction of the forces on particles 1 and 2, and the cosine of the bond-angle are computed. Finally, the force magnitude, $-dV(\theta)/d\theta$, and the forces on the particles are computed and then SCATTERed back into the force array.

Saving intermediate results of the calculations which do not change during the simulation will reduce the computational cost. Which quantities can be saved will depend on whether constraints are used. For example, the reciprocal of the sum of the masses for each 3-body force evaluation may always be saved. However, if the bond lengths are constrained, the normalization constants $1/\|\mathbf{r}_{31}\|^2$ and $1/\|\mathbf{r}_{32}\|^2$ may also be saved. Thus, constraining one intramolecular degree-of-freedom will reduce the cost of computing all others.

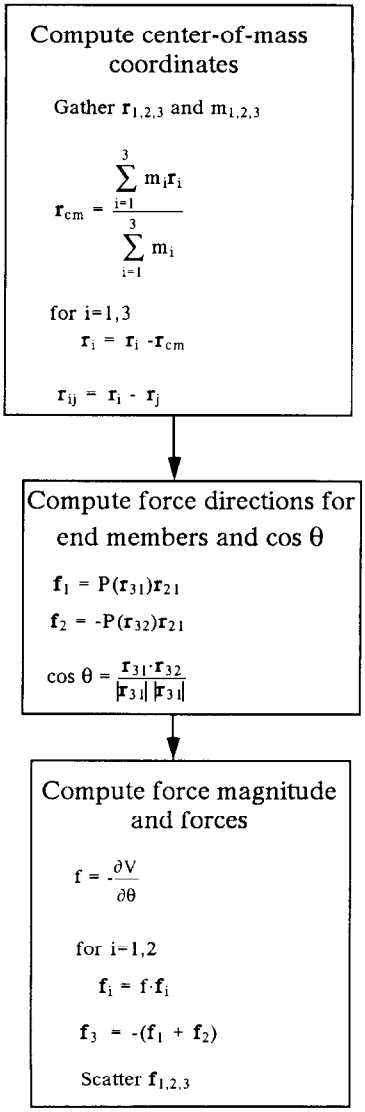

FIG. 4. Flowchart detailing bond-angle-bending algorithm.

B. *Torsion*

In the same way as angle-bending, the torsion algorithm consists of three phases (see Fig. 5). The center-of-mass coordinates are computed in the first phase. Next, the first set of projections and the cosine of the dihedral angle are computed. Finally, the force magnitude, $-dV(\phi)/d\phi$, and the forces on the particles are computed and then SCATTERed back into the force array.

Computational cost may be reduced by retaining intermediate results of the calculations. As with angle-bending, the reciprocal of the sum of the masses of the 4-body system can always be retained. If the bond lengths are constrained, the normalization constants, $1/\|\mathbf{r}_{ij}\|^2$, may be retained. If the bond-angles are constrained as well, the expressions $(\mathbf{r}_{32} \cdot \mathbf{r}_{21}/\|\mathbf{r}_{32}\|^2)$ and $(\mathbf{r}_{32} \cdot \mathbf{r}_{43}/\|\mathbf{r}_{32}\|^2)$ may be retained.

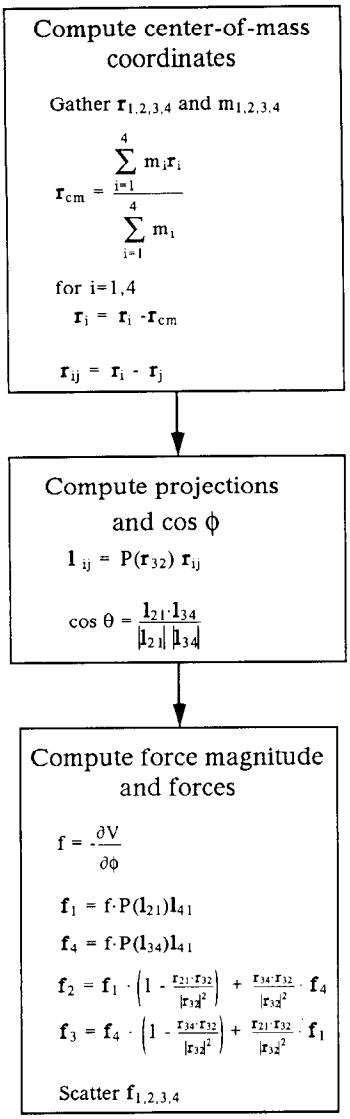

FIG. 5. Flowchart detailing torsion algorithm.

IV. TESTS

A. *Timing*

All codes were compiled using CFT77 and linked with SEGLDR on a Cray XMP-24. The Cray Assembly code version of BLAS [9] was used. The times per operation presented in Table I are based on simple subroutines that perform the indicated operation on pairs of vectors. Estimates for the relative execution times of the angle-bending and torsion codes are based on these values: we have not included the costs of GATHER and SCATTER operations, which are common to both codes, nor the operations necessary to calculate the magnitude of the force.

The estimated times of execution of the projection-based code for angle-bending are compared to those of the conventional cross-product code in Table II. The projection-based code is approximately seven times faster than the cross-product-based code. The two algorithms for torsion are compared in Table III, where it is seen that the projection method is approximately 2.5 times faster than the cross-product method. The projection-based algorithms derive their greater efficiency primarily from the use of fewer of the costly SQRT and divide functions.

TABLE I

Time per Operation

Operation	Time (ns)
SQRT	76
Divide	33
Multiply	15
SAXPY[a]	13
SDOT[b]	10

Note. Time per operation of arithmetic procedure required to calculate angle-bending and torsion forces.

[a] SAXPY(r, A, B) performs the operation $A(I) = A(I) + r * B(I)$.

[b] SDOT calculates the dot product of A and B.

TABLE II

Angle-Bending Force

Quantity	Required operations
	Projections
$\mathbf{f}_1$	2 dot products, 3 SAXPY, 1 divide
$\mathbf{f}_2$	2 dot products, 3 SAXPY, 1 divide
2 divides	66 ns
4 dot products	40 ns
6 SAXPY	78 ns
Total	122 ns
	Cross-products
$\|\mathbf{r}_{32}\|$	1 SQRT, 1 divide
$\|\mathbf{r}_{31}\|$	1 SQRT, 1 divide
$\mathbf{e}_{32}$	3 divides
$\mathbf{e}_{31}$	3 divides
$\mathbf{s}_1$	6 SAXPY, 2 divides, 6 multiplies
$\mathbf{s}_2$	6 SAXPY, 2 divides, 6 multiplies
2 SQRT	220 ns
12 divides	396 ns
12 multiplies	180 ns
12 SAXPY	157 ns
2 dot products	20 ns
Total	953 ns

Note. Time to calculate quantities required to evaluate angle-bending forces by projection and cross-product based methods.

TABLE III

Torsional Force

Quantity	Required operations
	Projections
l_{14}	1 SDOT, 3 SAXPY, 1 divide
l_{21}	1 SDOT, 3 SAXPY
l_{43}	1 SDOT, 3 SAXPY
$\mathbf{s}_1$	1 SDOT, 3 SAXPY, 1 divide
$\mathbf{s}_4$	1 SDOT, 3 SAXPY, 1 divide
$\mathbf{s}_2$	2 SAXPY
$\mathbf{s}_3$	2 SAXPY
$\cos\phi$	1 SDOT, 1 divide, 1 SQRT
1 SQRT	76 ns
4 divides	132 ns
15 SAXPY	185 ns
6 SDOT	60 ns
Total	453 ns
	Cross-products
$\|\mathbf{r}_{12}\|$	1 SQRT, 1 divide
$\|\mathbf{r}_{23}\|$	1 SQRT, 1 divide
$\|\mathbf{r}_{43}\|$	1 SQRT, 1 divide
$\mathbf{e}_{12}$	3 divides
$\mathbf{e}_{23}$	3 divides
$\mathbf{e}_{43}$	3 divides
$\mathbf{s}_1$	2 divides, 6 multiplies, 3 SAXPY
$\mathbf{s}_4$	2 divides, 6 multiplies, 3 SAXPY
$\mathbf{s}_2$	1 divide, 6 SAXPY
$\mathbf{s}_3$	1 divide, 6 SAXPY
$\cos^2\theta_2$	1 SDOT, 1 multiply
$\sin^2\theta_2$	1 subtraction
$\cos\phi$	1 SDOT
3 SQRT	228 ns
15 divides	495 ns
7 multiplies	105 ns
18 SAXPY	234 ns
5 SDOT	50 ns
Total	1112 ns

Note. Time to calculate quantities required to evaluate torsion forces by projection and cross-product methods.

CONCLUSIONS

We have analyzed the problem of efficiently computing angle-bending and torsion forces in molecular dynamics simulations. Our analysis concerns two aspects of this problem: (1) the inherent complexity of calculating angle-bending and torsion forces; and (2) how the nature of this complexity allows a general scheme for partitioning of the calculations for efficient vector computation. Further, given specific geometrical constraints, there is an additional increase in the efficiency of these calculations. The results of our comparisons demonstrate the efficiency of this approach.

ACKNOWLEDGMENTS

The authors extend special thanks to Gary Jones (DARPA Advanced Submarine Technology (AST) COTR for Hydrodynamics and Ship Control) and Dr. William Sandberg of NRL for their interest and support. This work was performed under ONR Contract N00014-88-WX-24087 with additional computational support provided by the Naval Research Laboratory Research Advisory Council and DARPA AST Contract MDA 972-88-C-0064.

REFERENCES

1. M. P. Allen and D. J. Tildesley, *Computer Simulation of Liquids* (Clarendon Press, Oxford, 1987).
2. E. B. Wilson, J. C. Decius, and P. C. Cross, *Molecular Vibrations* (McGraw–Hill, New York, 1955).
3. H. B. G. Casimir, *The Rotation of a Rigid Body in Quantum Mechanics* (Wolter, Leyden, 1931).
4. C. Eckart, *Phys. Rev.* **47**, 552 (1935).
5. S. G. Lambrakos, J. P. Boris, E. S. Oran, I. Chandrasekhar, and M. Nagumo, NRL Memorandum Report 6174, 1988 (unpublished).
6. S. G. Lambrakos, J. P. Boris, E. S. Oran, I. Chandrasekhar, and M. Nagumo, *J. Comput. Phys.* **85**, 473 (1989).
7. A. S. Householder, *The Theory of Matrices in Numerical Analysis* (McGraw–Hill, New York, 1958).
8. R. L. Hilderbrandt, *J. Mol. Spectrosc.* **44**, 599 (1972).
9. C. L. Lawson *et al.*, *Trans. Math. Software* **5**, 308 (1980).